

Interrelation between monopoles, vortices, topological charge, and chiral symmetry breaking: Analysis using overlap fermions for $SU(2)$

V. G. Bornyakov

¹*Institute for High Energy Physics, Protvino, 142281, Russia, and
Institute of Theoretical and Experimental Physics, B. Chermushkinskaya 25, Moscow, 117259, Russia*

E.-M. Ilgenfritz and M. Müller-Preussker

Humboldt-Universität zu Berlin, Institut für Physik, Newtonstrasse 15, 12489 Berlin, Germany

B. V. Martemyanov, S. M. Morozov, and A. I. Veselov

Institute of Theoretical and Experimental Physics, B. Chermushkinskaya 25, Moscow, 117259, Russia
(Received 31 August 2007; revised manuscript received 27 February 2008; published 25 April 2008)

We study the properties of configurations from which P-vortices on one hand or Abelian monopoles on the other hand have been removed. We find that the zero modes and the band of nonzero modes close to zero disappear from the spectrum of the overlap Dirac operator, confirming the absence of topological charge and quark condensate. The different behavior of the modified ensembles under smearing compared to the unmodified Monte Carlo ensemble corroborates these findings. The *gluonic* topological susceptibility rapidly approaches zero in accordance with $Q_{\text{index}} = 0$. The remaining (ultraviolet) monopoles without vortices and—to a less extent—the remaining vortices without monopoles are unstable under smearing whereas smearing of the unmodified Monte Carlo ensemble affects the monopoles and vortices only by smoothing, reducing the density only slightly.

DOI: [10.1103/PhysRevD.77.074507](https://doi.org/10.1103/PhysRevD.77.074507)

PACS numbers: 11.15.Ha, 11.10.Wx, 11.30.Rd, 12.38.Gc

I. INTRODUCTION

There are two popular phenomenological scenarios explaining confinement in lattice gluodynamics, monopole condensation [1], and the center vortex [2] mechanism. The basic ideas of both scenarios go back to 't Hooft [3,4]. Both have been recently discussed in Refs. [5,6]. For our discussion, monopoles and center vortices are defined by projection to Abelian $U(1)^{N-1}$ or $Z(N)$ gauge fields, respectively. In order to distinguish them from extended vortices, these $Z(N)$ center vortices are called P-vortices. The two types of excitations, when derived from the Maximally Abelian Gauge (MAG) or from the Maximal Center Gauge (MCG), respectively, reproduce about 90% [7] and about 70% [8] of the non-Abelian string tension. This observation is called monopole and center dominance. The monopole dominance should not be confused with Abelian dominance, which describes the fact that the projected degrees of freedom (the $U(1)^{N-1}$ valued links) reproduce the original string tension equally well. Without gauge fixing the full static potential is reproduced by Abelian projected or center projected links [9,10].

The importance of the topological excitations and of the corresponding MAG or MCG fixing, rests more on the physical reality of the excitations as the possibly relevant infrared degrees of freedom than on the monopole or P-vortex dominance. The reality is witnessed by their localization and the local excess of action and topological charge carried by monopoles and P-vortices. The infrared degrees of freedom could be used to derive effective theo-

ries to describe the infrared physics, for instance, the Dual Ginzburg-Landau theory [11]. This paper elaborates on some other aspects of the physical reality of monopoles and P-vortices. It turns out that they are constitutive also for other nonperturbative features besides confinement. Removing monopole degrees of freedom [12,13] or P-vortices [14–16] from the (lattice) fields should leave only inert and topologically trivial gauge field configurations.

For the issue of physical reality the conjecture [17,18] was very important that monopoles and P-vortices are geometrically interrelated. Indeed, this was found to be the case in $SU(2)$ gluodynamics. More than 90% of monopole currents are localized on the P-vortices [18–20]. The effect of eliminating one or the other, however, is more complicated and obviously destroys this geometrical interrelation.

It was realized that the removal of monopoles destroys only large (infrared) P-vortex clusters whereas the total density of P-vortex plaquettes is suppressed by less than an order of magnitude [21]. In the case of removal of vortices the total density of monopole links is even increased compared to the initial equilibrium configurations [21]. In that paper we have confirmed (for a finite temperature $T \approx 0.75T_{\text{dec}}$ in the confinement phase) that for the manipulated lattice ensembles confinement is missing. In particular, we were able to point out why the apparently percolating clusters of monopoles remaining after vortex removal cannot produce confinement. After this observa-

tion it is impossible to directly infer confinement from the existence of percolating monopoles.

In the present paper we turn our attention to the topological and chiral aspects of monopoles and vortices. The first new element in comparison with all previous studies of monopole removal and all but one paper on vortex removal is that we use chirally perfect overlap fermions [22,23] as a probe to confirm the loss of topological charge and the vanishing of the quark condensate in the modified ensembles obtained by monopole or vortex removal. The other new feature is that for the first time we employ an improved lattice gauge action in this kind of study. For all 50 configurations in the original and the modified ensembles we have determined 20 (in modulus) lowest eigenvalues λ_N and the corresponding eigenmodes (not used here) of the massless Neuberger overlap Dirac operator. To identify the topological charge we refer to the index of this Dirac operator. This is complemented by an improved gluonic expression for the topological density, leading to the same conclusion. We notice that the gluonic measurement of the topological charge requires a certain amount of APE smearing. This gives us the opportunity to investigate in what respect the modified ensembles differ from the original Monte Carlo one with respect to moderate smearing. For this part of our study an enlarged ensemble of 100 configurations has been used.

In Sec. II we give necessary information about the lattice ensembles that we have used. In Sec. III the effect of the removal of monopole, photon, and vortex degrees of freedom on the spectrum close to $\lambda_N = 0$ and on the topological charge is described. In Sec. IV we describe the behavior under smearing—concerning the measured monopole, vortex, and topological content—which is strikingly different between the equilibrium ensemble and the modified ensembles with monopoles and vortices removed. Section V contains our conclusions. In the Appendix all necessary definitions are collected.

II. SIMULATIONAL SETUP

In two previous papers [24,25] we have applied the overlap Dirac operator for $SU(2)$ lattice gauge theory in conjunction with the tree-level tadpole-improved Symanzik action. This will be the setup also here. The overlap construction [22,23] provides a perfectly chiral description for lattice fermions. The choice of action is motivated as follows. In our first paper [24] we have applied the overlap Dirac operator for a very specific investigation, to find evidence for a partially dyonic, partially caloronic structure of the topological charge distribution at $T = T_{\text{dec}}$. For this purpose it was essential to make sure that the configurations are smooth enough such that the number of zero modes and the gross structure of the spectrum of lowest overlap Dirac eigenvalues are robust with respect to a change of temporal boundary conditions and with respect to smearing. This would not be the

case for the Wilson action. For the tree-level tadpole-improved Symanzik action at high enough β_{imp} this requirement is fulfilled. This has determined us to work on a $20^3 \times 6$ lattice in the paper [24] where $\beta_{\text{imp},c} = 3.25$ has been found to be the deconfinement critical point. In a second paper [25] we have extended our investigation with this action to temperatures T below T_c and up to $2T_c$. Here our focus was the dependence of the spectral density and the localization behavior of the eigenmodes on the sign of the spatially averaged Polyakov loop L as soon as it ceases to vanish in the deconfined phase. In this paper it has been found that a gap opens in the spectral density for $T > 1.05T_{\text{dec}}$, but only for configurations with a positive spatially averaged Polyakov loop, $L > 0$, in agreement with predictions by Stephanov [26].

We refer to these two papers for details concerning the action and the implementation of the overlap Dirac operator. For the present investigation we have chosen the same lattice size $20^3 \times 6$ and the same action. We work at $\beta_{\text{imp},c} = 3.25$. There is no need to compare different boundary conditions. Now the overlap Dirac operator is uniquely endowed with antiperiodic boundary conditions in the temporal and periodic ones in the spatial directions. We have extended the ensemble to 50 configurations, that was begun with 20 configurations for Ref. [24]. The eigenvalues λ_{imp} of the improved Neuberger operator [27] are obtained by stereographic projection from λ_N situated on the Ginsparg-Wilson circle onto the imaginary axis, such that in the following the eigenvalues are understood as $\lambda \equiv \Im \lambda_{\text{imp}}$.

Since we have chosen to work at the deconfinement temperature, it makes no sense to discuss here once more the influence of the removal of monopoles or vortices on the string tension [21]. We are concentrating here on the effect of monopoles and vortices on the topological charge Q via the Atiyah-Singer index theorem [28],

$$Q = N_- - N_+, \quad (1)$$

with N_+ and N_- the number of zero modes of positive and negative chirality, and the spectral density $\rho(\lambda)$ near $\lambda = 0$, which is related via the Banks-Casher relation [29]

$$\langle \bar{\psi} \psi \rangle = -\frac{\pi \rho(0)}{V} \quad (2)$$

(with the four-volume $V = N_s^3 N_t a^4$) to the quark condensate. Whenever more than one zero mode is found for one configuration, the chirality of all of them is found to be the same.

For the ensemble of configurations at $T = T_{\text{dec}}$ in Ref. [24] the gross spectral density was seen to be independent of the boundary condition which means that it is insensitive also to the sign of the (very small) average Polyakov loop in our ensemble. This makes it possible to study the nontrivial effect of monopole or vortex removal on the spectral density in an unambiguous way.

The monopole line density [30] and the P-vortex plaquette density referred to later are defined in units of the lattice spacing as

$$\rho_{\text{mon}} a^3 = \frac{\langle N_{\text{mon}} \rangle}{4N_s^3 N_t} \quad \text{and} \quad \rho_{\text{vort}} a^2 = \frac{\langle N_{\text{vort}} \rangle}{6N_s^3 N_t}, \quad (3)$$

where N_{mon} is the number of dual links carrying nonvanishing monopole currents for an Abelian projected gauge field obtained from the MAG. N_{vort} is the number of dual plaquettes belonging to the total P-vortex area after applying the center projection to the gauge field put into the direct maximal center gauge (DMCG) [31]. More about these definitions and the procedures that lead to the detection and removal of monopoles and vortices can be found in the Appendix.

The following results concerning the density of monopoles and vortices and the investigation of the behavior under smearing in Sec. IV are based on an ensemble of 100 configurations.

At $T = T_{\text{dec}}$, for our equilibrium configurations the vortex density is found to be $\rho_{\text{vort}} a^2 = 0.0231(4)$. With the zero-temperature string tension $\sigma_0 = \sigma(T = 0)$ setting the scale, this corresponds to $\rho_{\text{vort}}/\sigma_0 = 0.417(8)$ or $\rho_{\text{vort}} = 2.08(4) \text{ fm}^{-2}$. This number is essentially smaller than the zero-temperature density found with the Wilson action to be about 4 fm^{-2} [32]. We think that this large difference is mostly due to difference in actions used in Ref. [32] and in this paper rather than due to finite temperature effects, i.e., it indicates that the vortex density with improved action is substantially smaller than with Wilson action.

The monopole density in the equilibrium ensemble amounts to $\rho_{\text{mon}} a^3 = 0.0117(1)$, that means $\rho_{\text{mon}}/\sigma_0^{3/2} = 0.897(9)$ or $\rho_{\text{mon}} = 10.0(1) \text{ fm}^{-3}$. For comparison, we recall an estimate [33] of the monopole density at $T = 0$ for $\beta_{\text{imp}} = 3.25$ and the same action: $\rho_{\text{mon}} a^3 = 0.0126(1)$. That means that the monopole density is only insignificantly suppressed at T_{dec} compared to $T = 0$.

These densities have to be taken with a grain of salt because it is known that they should be decomposed in an infrared and an ultraviolet part. The presence of both components becomes obvious in studies of universality [33] where only the infrared part possesses a finite continuum limit that can be compared between different actions. This problem will show up in the process of smearing discussed in Sec. IV.

The topological susceptibility of the equilibrium ensemble defined by $\langle Q_{\text{overlap}}^2 \rangle = 7.3 \pm 1.5$ translates to $\chi_{\text{top}}/\sigma_0^2 = 0.049 \pm 0.010$ or, assuming $\sqrt{\sigma_0} = 440 \text{ MeV}$, to $\chi_{\text{top}} = (207 \pm 10 \text{ MeV})^4$. This is in the right ballpark for the (unsuppressed) topological susceptibility. Once monopole or vortex degrees of freedom are removed from the configurations the fermionic (overlap) topological charge is strictly vanishing. It might come unexpectedly that Q_{overlap} is not preserved if the regular (photon) degrees of freedom are removed from the configurations. We will

point out later that in this case also the opposite (vanishing topological charge) could have been expected. For this modified ensemble $\langle Q_{\text{overlap}}^2 \rangle = 5.3 \pm 1.25$ has been measured.

III. THE SPECTRUM OF LOW-LYING MODES FOR CONFIGURATIONS WITH REMOVED MONOPOLES, PHOTONS, AND VORTICES

In this section we demonstrate the disappearance of the quark condensate and the complete loss of topological charge in modified ensembles of configurations having monopoles or vortices removed. We emphasize that this effect has been partly studied already [12–16], for either monopoles or vortices removed, with various gauge actions and fermionic actions (staggered, chirally improved) for the confinement phase. Thus, the results of this section are a confirmation of the crucial role of monopole and vortex degrees of freedom for the spectral properties obtained with a new, more convincing tool—the overlap Dirac operator. Let us note that results obtained at the edge of the confining phase of quenched $SU(2)$ gluodynamics are not less interesting. At this temperature the topological susceptibility is still approximately the same as for $T = 0$, and the spectral gap is not yet opened [25].

In Fig. 1 we illustrate this by one configuration. The panel on the extreme right shows the spectrum of low-lying modes of overlap fermions after removing the vortex degrees of freedom. This should be compared with the origi-

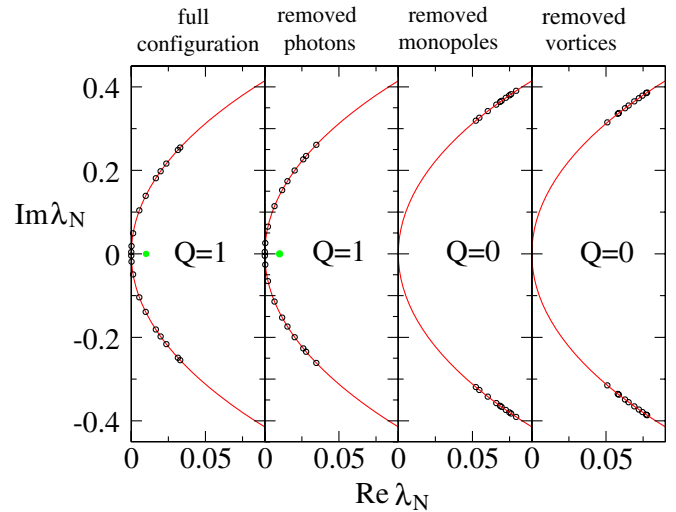


FIG. 1 (color online). The eigenvalues of the 20 lowest non-zero modes (open symbols) and the eventual zero mode (filled symbol) of the overlap Dirac operator lying on the Ginsparg-Wilson circle for one of the equilibrium configurations; for the original configuration (extreme left), the configuration with removed photon degrees of freedom (middle left), with removed monopole degrees of freedom (middle right), and with vortices removed (extreme right). The zero mode (green in online color) is pulled away from the Ginsparg-Wilson circle for better visibility of all modes.

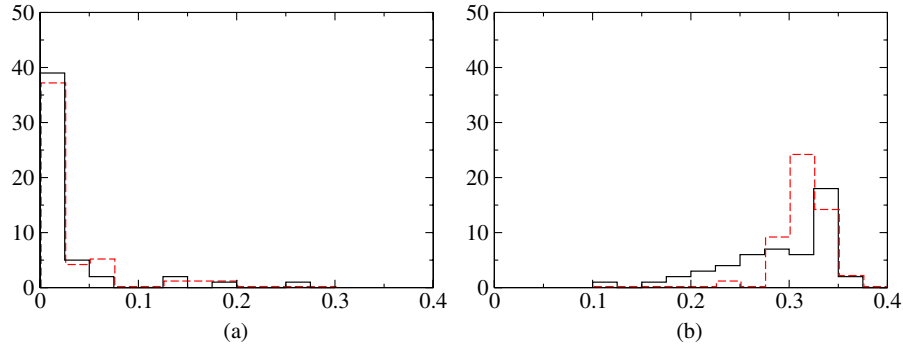


FIG. 2 (color online). The gap distributions (distributions of the first nonzero positive eigenvalue λ_1) for the four ensembles of 50 lattice configurations: (a) the original equilibrium configurations (solid line) and the configurations with removed photons (dashed line), (b) the configurations with removed monopoles (solid line) and with removed vortices (dashed line).

nal spectrum shown on the extreme left. The originally existent zero mode has disappeared, and the nonzero modes have moved outward. A similar change of the spectrum can be observed on the middle right panel after removing the monopole degrees of freedom from the same configuration. In the middle left panel the effect of removing the regular (photon) part from the Abelian projected field is shown. This spectrum differs only in minor details from the original spectrum, but the number of zero modes and the interval covered by the 20 modes remained un-

affected. We have to stress that the number of zero modes is not always stable with respect to the removal of the regular part of the Abelian field. The latter comparison enforces the conclusion that, from the point of view of Abelian projection, the decisive role for chiral symmetry breaking is played by the monopole part of the Abelian projected field, whereas the topological charge is not robust against the reduction of the Abelian field to its singular (monopole) part.

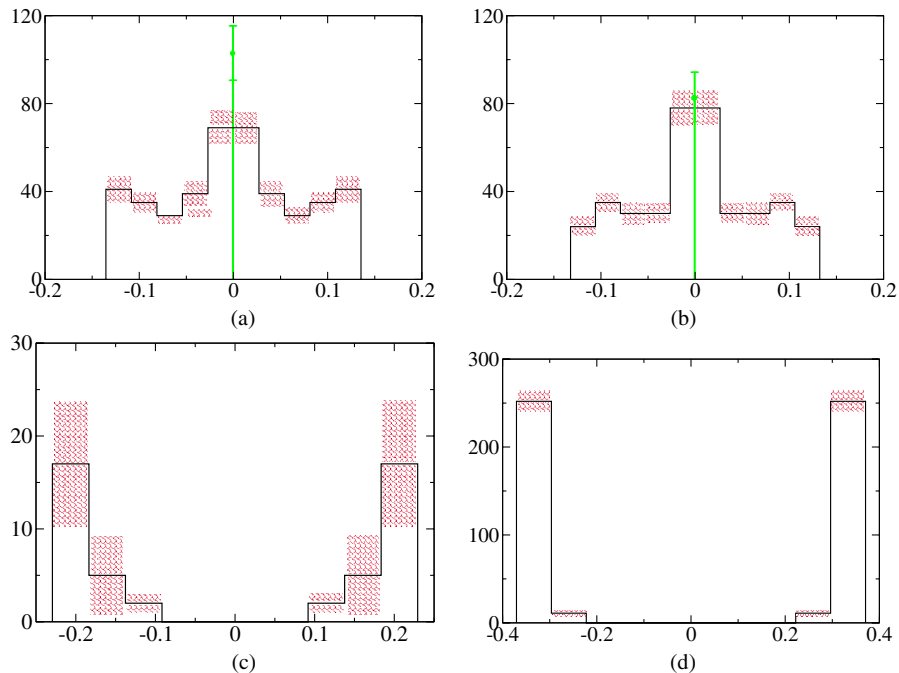


FIG. 3 (color online). The histogram of the eigenvalues λ for 20 lowest nonzero modes. The shadowing on top of the columns (red in color online) represents the statistical error. The total number of zero modes of the overlap Dirac operator is shown by the height of the spike (green in color online) drawn at zero. The plots show the four corresponding ensembles of 50 lattice configurations: (a) the original equilibrium configurations, (b) the configurations with removed photons, (c) the configurations with removed monopoles, and (d) with removed vortices. The spectra are shown in an interval defined by the minimum over 50 configurations of the largest (in modulus) of 20 individual configuration eigenvalues, thus eliminating the dependence of the shown part of the spectrum on the number of actually calculated eigenvalues.

In Fig. 2 we show the distribution of the first nonzero, positive eigenvalue λ for the four ensembles. After removing the regular part of the Abelian projected gauge field the distribution is only very minimally widened compared to the distribution of the original ensemble [see Fig. 2(a)]. After removing monopoles the distribution changes completely. It is rather wide with some tail towards $\lambda = 0$, but with a clear gap separating it from $\lambda = 0$, while the gap is wider and less fluctuating in the case of removed vortices [see Fig. 2(b)].

The respective average cumulated spectral densities as anticipated from all lowest 20 eigenmodes in our equilibrium ensemble of 50 configurations and the modified ensembles are shown as histograms in Fig. 3. The spike at zero shows the total number of zero modes in the ensemble of 50 configurations (irrespective of their chirality). The height corresponds to the scale of the embedding histogram. We see that zero modes and hence the topological charge completely disappear after monopoles (bottom left) or vortices (bottom right) are removed from the configurations while the spectral density is pushed outward. This effect is stronger if vortices are removed, less if monopoles are removed. The appearance of the gap among the near-zero modes signals the vanishing of the quark condensate which is still nonvanishing at the given temperature for the original ensemble (top left) and after the removal of the photon degrees of freedom (top right).

Notice that in all configurations the zero modes are neither completely preserved nor completely destroyed when the photon degrees of freedom are suppressed. All we can say here is that the number of zero modes is a less robust feature provided only the monopole degrees of freedom are kept. The number of zero modes in the equilibrium configurations, N_{equil} , and in the corresponding no-photon configurations, N_{nophot} , are strongly correlated. From the scatter plot of both numbers a regression formula, $N_{\text{equil}} = 0.15(25) + 0.77(10)N_{\text{nophot}}$, can be extracted. This finding might be difficult to reconcile with the notion of Abelian dominance of the topological charge [34,35]. Strict Abelian dominance of the latter would imply that after the removal of the regular “photon” part of the Abelian projected gauge field no topological charge should be left at all. These considerations were referring, however, to cooled configurations and the ground state whereas we consider here unsmearred configurations at nonzero temperature.

IV. SMEARING OF CONFIGURATIONS VOID OF MONOPOLES OR VORTICES

We can describe the interrelation between monopoles and P-vortices by the effect of removing one type of infrared degrees of freedom on the density of the other. We should emphasize again that the density alone does not decide about the confining property of the ensemble [21].

Here we are asking whether smearing is able to reveal that a lattice ensemble is corrupted in an essential way by the removal of monopoles or vortices. In the confinement phase “corrupted” means that it is unable to confine. We answer this question affirmatively without reference to the string tension showing that the density of complementary objects and the topological susceptibility disappear under smearing. We have seen already that the effect of vortex or monopole removal on the chirally perfect Dirac spectrum shows up without smearing. This does not change afterwards under the influence of smearing.

A. Vortices removed

Let us now consider the effect of removing P-vortices from the configurations performing the link operation (A11) on the monopole content and on the topological charge. At this step, the monopole density ρ_{mon} is approximately doubled to $\rho_{\text{mon}}a^3 = 0.0233(3)$. The abundant monopole lines form clusters that still contain a percolating component, but the non-Abelian string tension vanishes as it should [14]. Also the monopole string tension vanishes [21] in agreement with expectations. The unphysical (inert) character of magnetic monopoles in the configurations modified by vortex removal was thoroughly discussed in [21]. In essence, the monopole clusters were found to be decomposable into small monopole loops, such that the magnetic currents are screened at large distances.

The effect of vortex removal is presented by dotted lines in Fig. 4(a) for the monopole density, in Fig. 4(b) for the vortex density, and in Fig. 5 for the topological susceptibility.

The monopole density is initially even enhanced compared to the unmodified ensemble before it is quickly wiped out by smearing. In contrast to this, the monopole density in the unmodified ensemble is only slowly reduced by smearing (only 1 order of magnitude within five steps). This effect of smearing reflects mainly the elimination of ultraviolet monopole objects. These are small monopole loops that are either appended to large loops or separately existing. The extended infrared monopole clusters survive with ultraviolet loops stripped off. This can be called “smoothing of monopoles.”

The effect of vortex removal on the vortex density is demonstrated by a dotted line in Fig. 4(b). The vortex density reappears after one smearing step at a very low level before it is finally rapidly wiped out by smearing. In contrast to this, the vortex density in the unmodified ensemble is slowly reduced by smearing (only by a factor of 3 within five steps). This effect of smearing reflects mainly the straightening of the vortex surface due to elimination of ultraviolet objects (these are isolated bubbles and decorations added to extended surfaces) whereas large infrared objects survive.

In Fig. 5 the effect of vortex removal on the topological susceptibility as determined by the gluonic topological

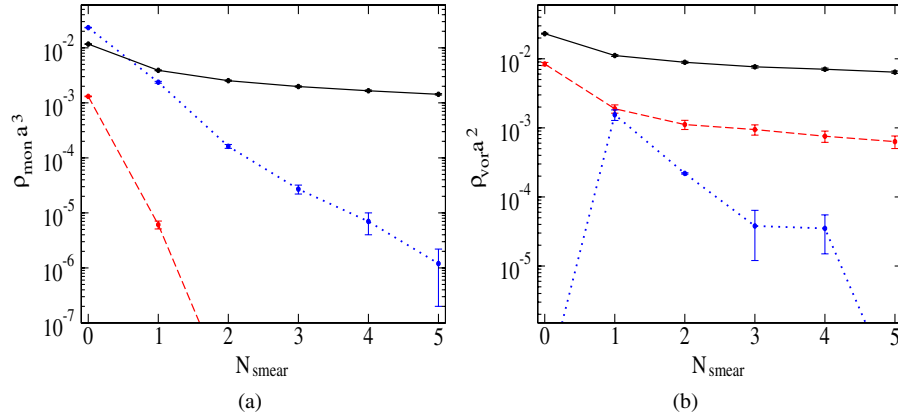


FIG. 4 (color online). The monopole density (a) and the vortex density (b) depending on the number of smearing steps for the original equilibrium ensemble of 100 configurations (solid lines) and for the modified ensembles differing by the removal of P-vortices (dotted lines) and the removal of monopoles (dashed lines).

density is also shown by a dotted line as a function of the smearing steps. More precisely, the susceptibility is quantified by the average of the topological charge squared $\langle Q_{\text{gluonic}}^2 \rangle$. In contrast to the original ensemble, where the topological susceptibility slowly approaches some final value from below, in the ensemble without vortices the (gluonic) topological susceptibility decays to zero within only five smearing steps.

For the gluonic topological charge density the topological susceptibility is known to receive additive and multiplicative renormalization [36]. Already few smearing steps show that the gluonic topological susceptibility becomes rapidly readjusted to zero in the modified ensemble without vortices for which the index of the overlap Dirac operator gives $Q_{\text{overlap}} = 0$ right from the beginning (before smearing starts). For this case the dotted curve in Fig. 5 resem-

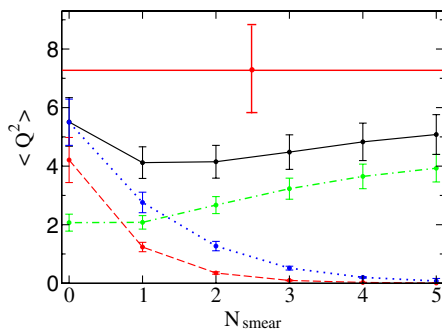


FIG. 5 (color online). The average of the gluonic topological charge squared, $\langle Q_{\text{gluonic}}^2 \rangle$, depending on the number of smearing steps for the original equilibrium ensemble of 100 configurations (solid line) and for the modified ensembles differing by the removal of P-vortices (dotted line), the removal of monopoles (dashed line), and the removal of photon degrees of freedom (dash-dotted line). The horizontal solid line above (with the statistical error bar) shows $\langle Q_{\text{overlap}}^2 \rangle$ for the unmodified equilibrium ensemble of 50 configurations (red in color online).

bles the additive renormalization constant of $\langle Q_{\text{gluonic}}^2 \rangle$ as a function of the number of smearing steps.¹

B. Monopoles removed

Next, let us describe what effect the removal of Abelian monopoles has on the P-vortex content in DMCG. The basic ensemble of configurations has been put into the MAG with the help of the simulated annealing method. The procedure of monopole removal is explained in Eqs. (A7)–(A10) in the Appendix.

We have put these lattice fields into DMCG and viewed the corresponding P-vortex content. The P-vortex plaquette density $\rho_{\text{vort}} a^2 = 0.0231(4)$ of the original ensemble, i.e., the total area of vortex plaquettes relative to the total number of plaquettes in the lattice, is reduced to $\rho'_{\text{vort}} a^2 = 0.0084(4)$ in the modified ensemble without monopoles. This amounts roughly to one third of the original density.

In the confinement phase, the contribution of the remaining center vortices to the quark-antiquark potential vanishes in the modified ensemble [21]. Here, the unphysical character of these leftover vortices is further elucidated by the smearing procedure as shown by the dashed line in Fig. 4(b). The vortex density decays but not more than by an order of magnitude.

If configurations modified by monopole removal are gauge-fixed again to MAG and Abelian projected, the number of monopole links that are then found is about 1 order of magnitude smaller than the number of monopoles defined for the original ensemble. The density of these artificial monopoles decreases extremely fast, by more than 2 orders of magnitude per smearing step, as shown by the dashed curve in Fig. 4(a).

¹The actual additive renormalization constant of the “field-theoretic topological density” should of course be measured on the subsample of $Q_{\text{overlap}} = 0$ original Monte Carlo configurations.

The effect of monopole removal on the topological susceptibility is much more pronounced. In Fig. 5 the dashed curve demonstrates that the gluonic estimator Q_{gluonic}^2 , which is immediately reduced before smearing, drops to zero within the first few smearing steps. The gluonic estimator is more strongly suppressed by a factor of 2 to 10 compared to the ensemble where P-vortices are removed. As we know, the fermionic topological charge is always $Q_{\text{overlap}} = 0$ as soon as monopoles have been removed.

For comparison we show in this figure also $\langle Q_{\text{overlap}}^2 \rangle$ obtained for the (unsmear) equilibrium ensemble from the index of the overlap Dirac operator, which we have found [24] to be stable under smearing. The value of $\langle Q_{\text{overlap}}^2 \rangle = 7.3 \pm 1.5$ is presented as the horizontal line. The gluonic estimator $\langle Q_{\text{gluonic}}^2 \rangle$ for the original ensemble continues to grow with smearing (not shown in Fig. 5 beyond $N_{\text{smear}} = 5$). The same tendency to rise towards the final, nonvanishing gluonic estimator $\langle Q_{\text{gluonic}}^2 \rangle$ we observe for the sample of photon-removed configurations. The fermionic value, $\langle Q_{\text{overlap}}^2 \rangle = 5.3 \pm 1.25$, is not yet reached.

V. CONCLUSIONS

In this paper, in order to clarify the role of certain $SU(2)$ gauge field excitations for the topological and chiral properties of the quenched ensemble of lattice fields, we have reconsidered the properties of the configurations at the deconfinement temperature $T = T_{\text{dec}}$ after removing two typical nonperturbative degrees of freedom. The condensation of the corresponding gauge field fluctuations, Abelian monopoles and center vortices (more precisely, P-vortices), is popularly held responsible for quark confinement at lower temperature. For our purpose we have applied special techniques of removal in order to study the effect on the complementary type of fluctuations and on the buildup of a topological charge and for the existence of a quark condensate. We confirm that for overlap quarks and also at the deconfinement temperature the suppression of each of these nonperturbative degrees of freedom leads to a loss of the complementary type of fluctuations, of topological charge, and chiral quark condensate. This effect is less pronounced for the loss of P-vortex density in the result of monopole suppression which might mean that the vortices, ceasing to percolate spatially at the deconfining temperature, become also decorrelated from the monopoles in the sense that they can exist also without monopoles. The converse is not true. The strength of this correlation is made visible by applying smearing.

Concerning the topological charge of a configuration we have the choice between an (improved) gluonic definition of Q_{gluonic} and the index of the overlap Dirac operator. While the fermionic topological charge Q_{overlap} is immediately destroyed by removing monopoles or vortices, the

gluonic topological susceptibility, in the absence of a true topological charge representing the additive renormalization for the topological susceptibility, rapidly drops to zero within a few smearing steps. For the unmodified ensemble, the actual topological charge Q_{overlap} (equal to plus or minus the number of zero modes) is insensitive with respect to smearing [24] even for more smearing steps than considered in this paper. This smearing usually makes visible extended topological background excitations, as, for example, calorons or BPS monopoles (dyons). These are suppressed as soon as Abelian monopoles or P-vortices are removed from the configurations such that no smearing can make them reappearing.

Finally we stress that, without any exception, quark condensation is impossible without monopoles and P-vortices. This is seen by inspecting the spectra of the overlap Dirac operator. While differing in details, a gap is opened if monopoles or vortices are removed. No gap is opening and almost all zero modes are preserved if only the photon degrees of freedom are eliminated from the Abelian projection.

ACKNOWLEDGMENTS

The work of ITEP group is partially supported by RFBR Grant Nos. RFBR 05-02-16306a and RFBR 07-02-00237a, and by No. RFBR 06-02-04010 together with DFG Grant No. 436 RUS 113/739/2. The work of E.-M. I. is supported by DFG through the Forschergruppe FOR 465 (Mu932/2).

APPENDIX

For self-contained readability of this paper we give the standard definitions for $SU(2)$ lattice gauge theory which we have used in the studies described in the text. We perform our analyses in the Direct Maximal Center Gauges. The DMCG in $SU(2)$ lattice gauge theory is defined by the maximization of the functional

$$F_U^{\text{DMCG}}(g) = \sum_{x,\mu} (\text{Tr}^g U_{x,\mu})^2, \quad (\text{A1})$$

with respect to gauge transformations $g \in SU(2)$. $U_{x,\mu} = \{U_{x,\mu}^{jk}\}$ ($j, k = 1, 2$) is the lattice gauge field and ${}^g U_{x,\mu} = g^\dagger(x) U_{x,\mu} g(x + \hat{\mu})$ the gauge-transformed one. Maximization of (A1) fixes the gauge up to $Z(2)$ gauge transformations, and the corresponding projected $Z(2)$ gauge field is defined as

$$Z_{x,\mu} = \text{sign}(\text{Tr}^g U_{x,\mu}). \quad (\text{A2})$$

After this identification is made, one can make use of the remaining $Z(2)$ gauge freedom in order to maximize the $Z(2)$ gauge functional

$$F_Z^{Z(2)}(z) = \sum_{x,\mu}^z Z_{x,\mu} \quad (\text{A3})$$

with respect to gauge transformations $z(x) \in Z(2)$, $z_{x,\mu} = z^*(x)Z_{x,\mu}z(x + \hat{\mu})$. This is the $Z(2)$ equivalent of the Landau gauge. In distinction to Ref. [14], this final step is automatically understood here before the vortex removal operation (to be defined below) is done. The $Z(2)$ gauge variables are used to form $Z(2)$ plaquettes. The P-vortex surfaces are actually formed by plaquettes *dual* to the negative plaquettes.

The Maximally Abelian Gauge is fixed by maximizing the functional

$$F_U^{\text{MAG}}(g) = \sum_{x,\mu} \text{Tr}(g U_{x,\mu} \sigma_3 (g U_{x,\mu})^\dagger \sigma_3), \quad (\text{A4})$$

with respect to gauge transformations $g \in SU(2)$. The maximization fixes the gauge up to $g \in U(1)$. Therefore, the following projection to an $U(1)$ gauge field through the phase of the diagonal elements of the links, $\theta_{x,\mu} = \arg(g U_{x,\mu}^{11})$, is subject to a remaining $U(1)$ gauge freedom. The non-Abelian link field is split according to $U_{x,\mu} = u_{x,\mu} V_{x,\mu}$ in an Abelian (diagonal) part $u_{x,\mu} = \text{diag}\{\exp(i\theta_{x,\mu}), \exp(-i\theta_{x,\mu})\}$ and a coset part $V_{x,\mu} \in SU(2)/U(1)$, the latter representing nondiagonal gluons.

In order to fix the MAG and the DMCG we have created 10 randomly gauge transformed copies of the original gauge field configuration and applied the simulated annealing algorithm [7] to find the optimal non-Abelian gauge transformation g .

We have used the standard DeGrand-Toussaint definition [37] of monopole currents defined by the phase $\theta_{x,\mu}$ of $u_{x,\mu}$. The part of the Abelian gauge field originating from the monopoles is

$$\theta_{x,\mu}^{\text{mon}} = -2\pi \sum_{x'} D(x - x') \partial'_\nu m_{x',\nu\mu}. \quad (\text{A5})$$

Here $D(x)$ is the inverse lattice Laplacian, and ∂'_μ is the lattice backward derivative. The Dirac sheet variable, $m_{x,\mu\nu}$, is defined by the integer part (modulo 2π) of the plaquette angle $\theta_{x,\mu\nu}$, whereas the reduced plaquette angle $\bar{\theta}_{x,\mu\nu} \in (-\pi, \pi]$ is the fractional part: $\theta_{x,\mu\nu} = 2\pi m_{x,\mu\nu} + \bar{\theta}_{x,\mu\nu}$. The photon part is

$$\theta_{x,\mu}^{\text{phot}} = \theta_{x,\mu} - \theta_{x,\mu}^{\text{mon}}. \quad (\text{A6})$$

The Abelian gauge field without monopole degrees of freedom is defined as [13]

$$u_{x,\mu}^{\text{monopole removed}} = (u_{x,\mu}^{\text{mon}})^\dagger u_{x,\mu}, \quad (\text{A7})$$

where $u_{x,\mu}^{\text{mon}} = \text{diag}\{\exp(i\theta_{x,\mu}^{\text{mon}}), \exp(-i\theta_{x,\mu}^{\text{mon}})\}$. Correspondingly, the Abelian gauge field without the photon degrees of freedom is simply the monopole part

$$u_{x,\mu}^{\text{photon removed}} = u_{x,\mu}^{\text{mon}}. \quad (\text{A8})$$

Upon multiplication with the coset field $V_{x,\mu}$, this holds also for the non-Abelian links without monopoles

$$U_{x,\mu}^{\text{monopole removed}} = (u_{x,\mu}^{\text{mon}})^\dagger U_{x,\mu} \quad (\text{A9})$$

and without photons

$$U_{x,\mu}^{\text{photon removed}} = (u_{x,\mu}^{\text{phot}})^\dagger U_{x,\mu}. \quad (\text{A10})$$

Analogously the non-Abelian gauge fields without P-vortices are defined as in Ref. [14]:

$$U_{x,\mu}^{\text{vortex removed}} = Z_{x,\mu} U_{x,\mu}, \quad (\text{A11})$$

where $Z_{x,\mu}$ is given by (A2).

Smearing is defined as an iterative field transformation with one step

$$U_{x,\mu}^{(n+1)} = \mathcal{P} \left\{ (1 - \alpha) U_{x,\mu}^{(n)} + \frac{\alpha}{6} \sum_{\nu, \nu \neq \mu} (U_{x,\nu}^{(n)} U_{x+\hat{\nu},\mu}^{(n)} U_{x+\hat{\mu},\nu}^{(n)\dagger} + U_{x-\hat{\nu},\nu}^{(n)\dagger} U_{x-\hat{\nu},\mu}^{(n)} U_{x-\hat{\nu}+\hat{\mu},\nu}^{(n)}) \right\} \quad (\text{A12})$$

where \mathcal{P} denotes the projection to $SU(2)$. This procedure has been used here to demonstrate the unphysical nature of monopoles, vortices, and gluonic topological charge apparently left over after the configurations have been modified by monopole/vortex removal. In the equilibrium ensemble, in contrast, these quantities are stable (up to changing renormalization) with respect to smearing, and the fermionic topological charge does not change at all. In this paper the smearing parameter has been set equal to $\alpha = 0.5$.

The gluonic definition of the topological charge density is based on the 3-loop $O(a^4)$ improved field strength tensor [38]

$$F_{\mu\nu}(x) = \left\{ \frac{1}{4} \sum_{\text{clover}} \left(\frac{3}{2} C_{\mu\nu}^{(1)}(x) - \frac{3}{20} C_{\mu\nu}^{(2)}(x) + \frac{1}{90} C_{\mu\nu}^{(3)}(x) \right) \right\}_{\text{traceless}}, \quad (\text{A13})$$

where the ‘‘clover’’ average is taken over the four untraced, oriented Wilson loops $C^{(R)}(x)$ of size $R \times R$ in the $\mu\nu$ plane that are touching each other in site x where they begin and end. The gluonic topological charge is then

$$Q_{\text{gluonic}} = \frac{1}{16\pi^2} \sum_x \sum_{\mu\nu\rho\lambda} \varepsilon_{\mu\nu\rho\sigma} \text{Tr}(F_{\mu\nu}(x) F_{\rho\sigma}(x)). \quad (\text{A14})$$

- [1] H. Shiba and T. Suzuki, Phys. Lett. B **333**, 461 (1994).
- [2] L. Del Debbio, M. Faber, J. Greensite, and S. Olejnik, Phys. Rev. D **55**, 2298 (1997).
- [3] G. 't Hooft, Nucl. Phys. **B138**, 1 (1978).
- [4] G. 't Hooft, Nucl. Phys. **B190**, 455 (1981).
- [5] J. Greensite, Prog. Part. Nucl. Phys. **51**, 1 (2003).
- [6] J. Greensite and R. Alkofer, J. Phys. G **34**, S3 (2007).
- [7] G. S. Bali, V. Bornyakov, M. Müller-Preussker, and K. Schilling, Phys. Rev. D **54**, 2863 (1996).
- [8] V. G. Bornyakov, D. A. Komarov, and M. I. Polikarpov, Phys. Lett. B **497**, 151 (2001).
- [9] M. C. Ogilvie, Phys. Rev. D **59**, 074505 (1999).
- [10] M. Faber, J. Greensite, and S. Olejnik, J. High Energy Phys. 01 (1999) 008.
- [11] Y. Koma, M. Koma, E.-M. Ilgenfritz, T. Suzuki, and M. I. Polikarpov, Phys. Rev. D **68**, 094018 (2003).
- [12] O. Miyamura, Phys. Lett. B **353**, 91 (1995).
- [13] S. Sasaki and O. Miyamura, Nucl. Phys. B, Proc. Suppl. **63**, 507 (1998); Phys. Lett. B **443**, 331 (1998).
- [14] P. de Forcrand and M. D'Elia, Phys. Rev. Lett. **82**, 4582 (1999).
- [15] J. Gattnar, Ch. Gatttringer, K. Langfeld, H. Reinhardt, A. Schäfer, St. Solbrig, and T. Tok, Nucl. Phys. **B716**, 105 (2005).
- [16] F. V. Gubarev, S. M. Morozov, M. I. Polikarpov, and V. I. Zakharov, JETP Lett. **82**, 343 (2005).
- [17] J. M. Cornwall, Phys. Rev. D **61**, 085012 (2000); **65**, 085045 (2002).
- [18] J. Ambjorn, J. Giedt, and J. Greensite, J. High Energy Phys. 02 (2000) 033.
- [19] A. V. Kovalenko, M. I. Polikarpov, S. N. Syritsyn, and V. I. Zakharov, Nucl. Phys. B, Proc. Suppl. **129**, 665 (2004).
- [20] A. V. Kovalenko, M. I. Polikarpov, S. N. Syritsyn, and V. I. Zakharov, Phys. Rev. D **71**, 054511 (2005).
- [21] P. Yu. Boyko, V. G. Bornyakov, E.-M. Ilgenfritz, A. V. Kovalenko, B. V. Martemyanov, M. Müller-Preussker, M. I. Polikarpov, and A. I. Veselov, Nucl. Phys. **B756**, 71 (2006).
- [22] H. Neuberger, Phys. Lett. B **417**, 141 (1998).
- [23] H. Neuberger, Phys. Lett. B **427**, 353 (1998).
- [24] V. G. Bornyakov, E.-M. Ilgenfritz, B. V. Martemyanov, S. M. Morozov, M. Müller-Preussker, and A. I. Veselov, Phys. Rev. D **76**, 054505 (2007).
- [25] V. G. Bornyakov, E. V. Lushchevskaya, S. M. Morozov, M. I. Polikarpov, E.-M. Ilgenfritz, and M. Müller-Preussker, Proc. Sci. LAT2007 (2007) 315 [arXiv:0710.2799].
- [26] M. A. Stephanov, Phys. Lett. B **375**, 249 (1996).
- [27] S. Capitani, M. Göckeler, R. Horsley, P. E. L. Rakow, and G. Schierholz, Phys. Lett. B **468**, 150 (1999).
- [28] M. F. Atiyah and I. M. Singer, Bull. Am. Math. Soc. **69**, 422 (1963).
- [29] T. Banks and A. Casher, Nucl. Phys. **B169**, 103 (1980).
- [30] V. G. Bornyakov, E.-M. Ilgenfritz, M. L. Laursen, V. K. Mitryushkin, M. Müller-Preussker, A. J. van der Sijs, and A. M. Zadorozhnyi, Phys. Lett. B **261**, 116 (1991).
- [31] L. Del Debbio, M. Faber, J. Giedt, J. Greensite, and S. Olejnik, Phys. Rev. D **58**, 094501 (1998).
- [32] F. V. Gubarev, A. V. Kovalenko, M. I. Polikarpov, S. N. Syritsyn, and V. I. Zakharov, Phys. Lett. B **574**, 136 (2003).
- [33] V. G. Bornyakov, E.-M. Ilgenfritz, and M. Müller-Preussker, Phys. Rev. D **72**, 054511 (2005).
- [34] V. G. Bornyakov and G. Schierholz, Phys. Lett. B **384**, 190 (1996).
- [35] S. Sasaki and O. Miyamura, Phys. Rev. D **59**, 094507 (1999).
- [36] M. Campostrini, A. Di Giacomo, H. Panagopoulos, and E. Vicari, Nucl. Phys. **B329**, 683 (1990); M. Campostrini, A. Di Giacomo, and H. Panagopoulos, Phys. Lett. B **212**, 206 (1988).
- [37] T. A. DeGrand and D. Toussaint, Phys. Rev. D **22**, 2478 (1980).
- [38] S. O. Bilson-Thompson, D. B. Leineweber, and A. G. Williams, Ann. Phys. (N.Y.) **304**, 1 (2003).